Effect of Geometry on the Performance of Model Metal Matrix Composite Joints and Transitions

D.D. Brink, S.A. Waltner, C.G. Levi, and F.A. Leckie

(Submitted 13 January 2000)

The role of geometry in the mechanical performance of various configurations of joints and transitions in metal matrix composites (MMCs) was investigated. Three types of model joints were manufactured by pressure infiltration of molten Al-4.5% Mg into preforms of continuous polycrystalline alumina fibers. This method of fabrication allows metal continuity to be achieved throughout the joint region, creating composite/monolith interfaces free of the gross defects that commonly limit joint strength. Test results indicate that changes in joint configuration affect the level of plastic flow at the composite/monolith interfaces, and suggest that increasing the level of plastic constraint in these regions enhances performance. The factors controlling interface behavior in the various joint configurations were investigated with finite element techniques, based on constitutive behavior measured experimentally. Using these methods, the evolution of the stress state which develops at the composite/monolith interfaces was probed, providing insight into the interplay between the state of stress and the failure mechanisms that limit interface performance. With this in mind, the relationship between key components of stress and the mechanical performance of the experimental specimens is discussed with respect to debonding and void growth at the composite/monolith interface.

Keywords finite element analysis, interface, joining, MMC, transition

1. Introduction

Metals reinforced with continuous fibers offer superior specific strength and stiffness—properties that are attractive in many applications. However, material anisotropy combined with uncertainties in interface properties makes these materials difficult to join, fostering overly conservative joint designs based largely on load transfer through shear. Oversize joints that detract from the weight saving benefits of the metal matrix composites (MMC's) are a consequence of this design philosophy. A better understanding of the behavior of composite/composite and composite/monolithic interfaces present in various joint geometries should enable the development of more efficient joint designs. The present paper focuses on the influence of geometry on the degree of metal constraint and the performance of composite/monolith interfaces. This research is part of a broader project aimed at elucidating the issues that control the load carrying ability of interfaces involving fiber terminations at the joint.

Investigations have hinged on the manufacture and testing of various configurations of model joints and transitions, shown schematically in Fig. 1. In addition, the experimental effort has been complemented by finite element analysis of the different geometries. As described in detail elsewhere,[1] the joints are fabricated by pressurized infiltration of molten Al alloys into preforms of continuous Al_2O_3 fibers, adjacent to either another preform or an open cavity as dictated by the desired geometry. In this process, the metal in the fiber composite and the adjacent structures are formed simultaneously, achieving continuity of the metal at the interface which minimizes defects common to conventional joining methods.[2] The mechanical performance of these samples should thus define a baseline against which other joints can be compared. In the current work, the matrix of the fiber composite and the adjacent metal consist of Al-4.5% Mg.

The general features of the mechanical behavior of the model butt joints (Fig. 1a) are discussed in Ref 3. Briefly, joint failure occurs consistently along the composite/interlayer interface *via* a mechanism involving debonding of the fiber tips, followed by linkage of the ensuing "cracks" by ductile tearing of the metal ligaments between them. Debonding, in turn, appears to involve microvoid nucleation and coalescence at the fiber tip/metal interface. Failure in the other specimen types (Fig. 1b, and c) shares many similarities with the butt joints. Initiation occurs at the composite/monolith interface and appears to depend heavily on the level of plasticity that develops in the region of the interface. Interface separation follows in a manner consistent with the above description and, in the case of the taper transition in Fig. 1(c), leads to shear failure along the length *l*. The applied load at which interface fracture occurs, however, is strongly dependent on the specimen type and appears to increase for geometries in which plastic flow is reduced near the composite/monolith interface.

Previous analytical and finite element models have been developed which describe the stress state within the interlayers of model butt joints, revealing large hydrostatic stresses in the interlayer center and elevated plastic strains near the free edge.[1,2]. The presence of these large hydrostatic stresses and

D.D. Brink, Materials Department, **S.A. Waltner** and **F.A. Leckie**, Department of Mechanical and Environmental Engineering, and **C.G. Levi**, Materials Department and Department of Mechanical and Environmental Engineering, The University of California at Santa Barbara, Santa Barbara, CA 93106. Contact e-mail: leckie@engineering.ucsb.edu.

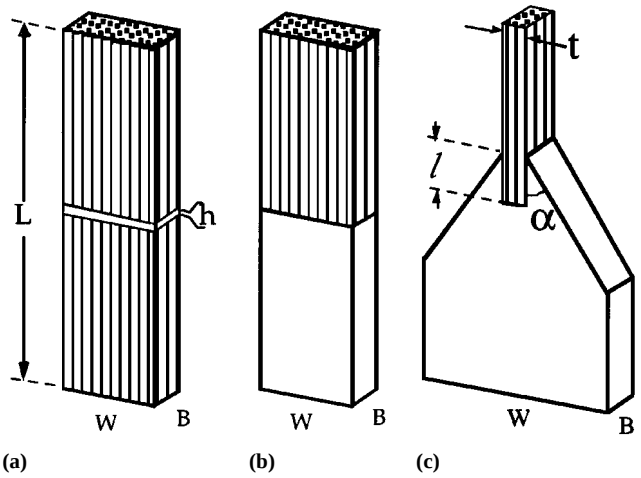

Fig. 1 Schematic depicting the various geometries investigated. These are the (**a**) butt joint, (**b**) simple transition, and (**c**) taper transition. The different configurations consist of a continuous fiber reinforced MMC adjacent to monolithic metal, creating an interface whose behavior is critical to joint performance

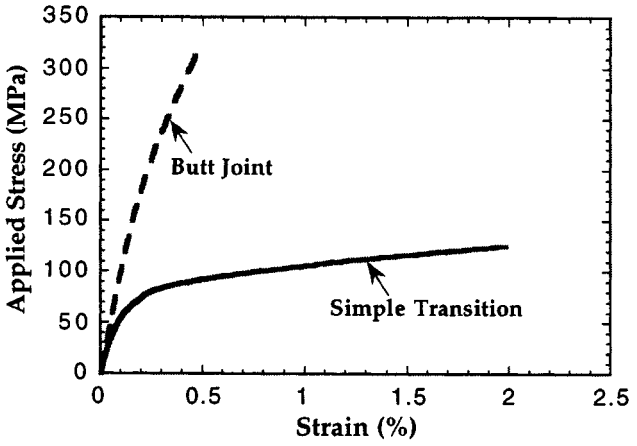

Fig. 2 Comparison of the mechanical response between the interlayer of the butt joint and the metal constituent of the simple transition. The higher stiffness and strength of the butt joint stem from the large degree of metal constraint in the interlayer

plastic strains is likely to influence interfacial failure by affecting the initiation and growth of interfacial voids.[4] In the current work, the dependence of these stresses on specimen geometry is explored by extending finite element modeling to the transition geometries. The evolution of the interfacial stress state is then probed to uncover the reasons behind the increase in mechanical performance associated with geometric changes that act to constrain plastic flow.

2. Experimental Testing and Failure Observations

The mechanical performance of the specimens was evaluated in tension by loading along the fiber direction. Figure 2 compares the behavior of the butt joint to that of the simple transition and is representative of five separate butt joints and two simple transition specimens. In the case of the butt joint, interlayer strain was measured experimentally in the longitudinal direction using a strain gage which spanned the joint.[1] Due to large strain gradients near the interface of the simple transition specimen, the strain was measured in a remote region of the aluminum and thus compares with the response of the monolithic material. The width and breadth of both the butt joint and simple transition specimens are approximately 6 and 4 mm, respectively. The length of both sample types is 3 in. In addition, the thickness of the butt joint interlayer is 160 μm, giving an aspect ratio B/h of ~25.

As evident in the figure, the mechanical response of the butt joint is stiffer than that of the simple transition, exhibiting apparent modulus values of 100 GPa and 70 GPa, respectively. In addition, the butt joint demonstrates a higher load carrying capacity than the transition. Indeed, the failure stress of the butt joint exceeds 300 MPa, far greater than the 130 MPa failure load of the simple transition specimen. Moreover, the strength of the butt joint is greater than the ultimate tensile strength (UTS) of the monolithic aluminum, which reaches a value of 190 MPa at ~9% strain.[1] The differences in behavior stem from the large amount of constraint imposed on the interlayer of the butt joint by the composite subelements. Briefly, shear forces which develop at the composite/interlayer interface restrict the inward contraction of the metal at the outer perimeter, causing large hydrostatic stresses to develop within the interlayer. Due to the in-plane components of the hydrostatic stress, a higher applied load is required to reach the yield criterion of the interlayer, allowing the constrained material to support higher loads than the monolithic metal. This effect is explored more fully in Ref 1.

Failure in the butt joints occurs by separation at the interface between the fiber composite and the metal interlayer. Evidence of interface failure can be seen in Fig. 3, which shows the macroscopic features of fracture in a butt joint. The darker regions of the micrograph correspond to exposed fiber ends and the lighter regions to the metallic interlayer. Note that the dark, fiber-side regions on the left side of the fracture surface match with the light, metal-side regions on the right side and *vice versa*. The patchy surfaces suggest that cracks initiate and grow at multiple sites on both sides of the interlayer, combining at later stages of fracture by metal shear in the interlayer.

Details of the fracture are shown in Fig. 4, revealing exposed fiber tips in (a) which appear to have debonded from sockets such as those shown on the metal side (b). The ductile tearing of the ligaments between the fibers suggests that the debonded fiber ends subsequently coalesced to form larger interfacial cracks, which, in turn, grow through further coalescence until a defect of critical size is reached. The appearance of the fracture on this scale is consistent across the surface of the butt joint, with the exception of preferential shearing of the metal ligaments in the perimeter region toward the center of the specimen.

Failure in the simple transitions is consistent with the butt joints in that it occurs at the interface between the composite

[1]This process is described in detail in Ref 3. In addition, the accuracy of this approach has been verified both with finite element models and *via in-situ* optical measurements of interlayer displacements.[5]

and monolithic aluminum. There is much less constraint in the simple transition, however, allowing more plasticity at the perimeter of the interface. Evidence of this plastic shear is seen in Fig. 5, which shows a close-up of the fracture near the sample edge. The extensive plastic deformation extends approximately 100 μm toward the specimen center, after which point the morphology of the fracture surface resembles the fiber end/socket pattern seen in the butt joints. The substantial amount of plastic flow in the perimeter region appears to have caused the initiation and coalescence of voids at the interface, suggesting that failure initiates at the free edge for this geometry.

The taper transition is more complex than either the butt joint or the simple transition, as load transfer occurs through shear along the length l as well as across the interface normal to the applied load. The overall length of these specimens is consistent with the other joints, although the thickness, t, is smaller at ~2 mm and the width, W, is larger at ~2.5 cm. The transition angle, α, is 30° in all cases. The relative amounts of shear to normal load transfer in the taper transition are dictated by the ratio of the shear length, l, to the composite thickness, t. The effects of l/t on the mechanical performance of taper transitions fall outside the scope of the current paper but will be considered in a subsequent publication.[6] The mechanical response of a sample with $l/t = 2$, shown in Fig. 6, is sufficient to show the relevant features of this geometry. As there is no meaningful single measure of strain for the taper transition, the figure depicts the applied load in the composite as a function of displacement.

The load carrying ability of the taper transition is superior to that of the other configurations at 390 MPa. This is due in large part to the shear load transfer along l, but also stems from the additional interfacial constraint provided by the metal in the taper regions. Notwithstanding the shear load contributions, the peak stress is limited by debonding of the interface normal to the applied load. *In-situ* optical observations with a charge coupled device (CCD) camera indicate that debonding is initiated at the corners of the fiber composite, presumably in regions

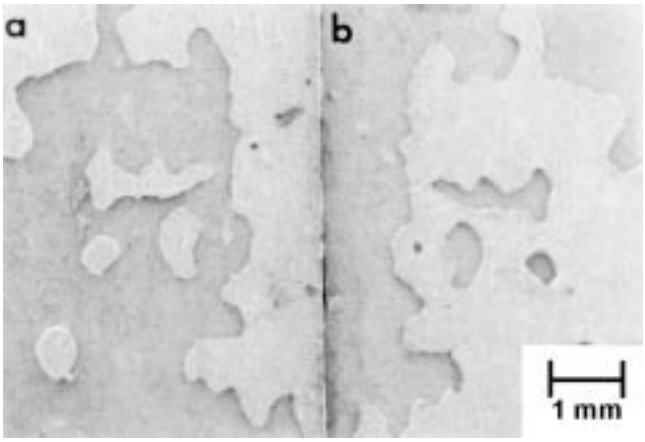

Fig. 3 (**a**) and (**b**) Overview of the fracture surface of a butt joint revealing separation of the composite/metal interface. The dark regions are representative of exposed fiber tips, while the lighter areas of the photo reflect the metal interlayer. Note the one-to-one correspondence between the light and dark regions on opposite sides of the fracture surface

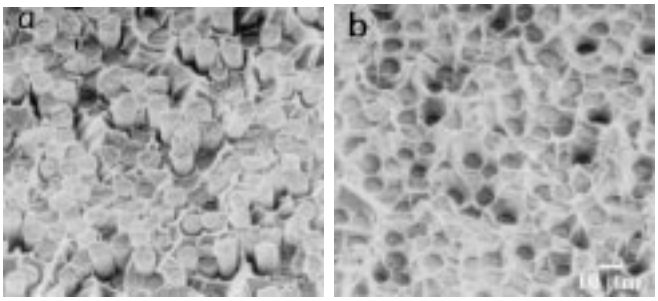

Fig. 4 Details of the fracture surface of a butt joint. The fiber tips on the side (**a**) have debonded from sockets on the metal side in (**b**). The subsequent coalescence of the debonded regions results in ductile tearing of the ligaments between the fibers

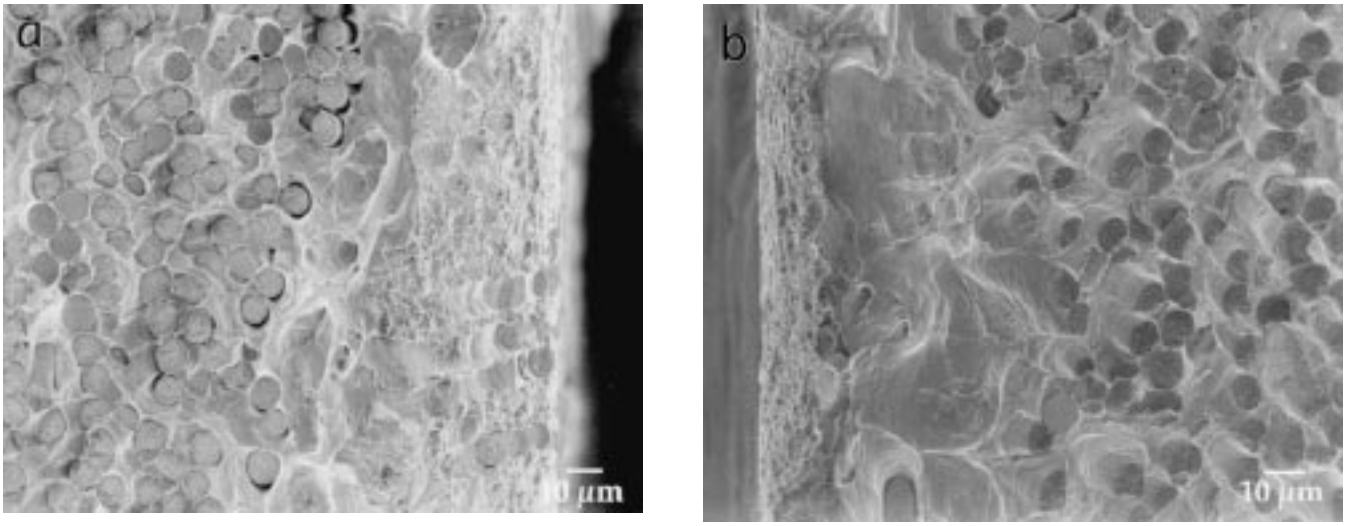

Fig. 5 Details of the fracture surface of the simple transition near an edge. Note the large amount of plasticity at the edge, after which point a correspondence between (**a**) the fiber tips on the composite side and (**b**) the sockets on the metal side is evident

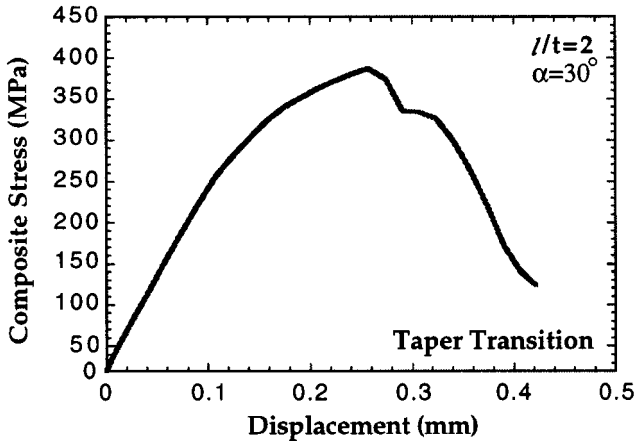

Fig. 6 Mechanical response of a taper transition with insertion ratio = 2. Since there is no meaningful measure of strain in the taper transition, the applied load in the composite is plotted as a function of displacement. Note that the sample reaches an applied load of 390 MPa significantly higher than that of the other geometries

of high plastic flow, then propagates across the remainder of the interface. Following debonding, the composite shears out from the monolithic section, creating the characteristic tail observable in Fig. 6.

The overall fracture of the taper transition is shown in Fig. 7(a) and clearly depicts separation of the composite and monolithic metal. Note that failure of the metal taper region was initiated at a small ceramic pin used to secure the preform during processing and is not characteristic of the geometry at the insertion ratio (*l*/*t*) shown. A closer view of the fracture surface in the region of the upper corner is shown in Fig. 7(b). Plastic flow in this area is delineated by the bent machining lines on the sample surface, and is consistent with optical observations during testing. Grooves formed during pullout of the fiber composite are evident on the right side of the micrograph, while the adjacent surface consists of the fiber socket morphology common to the butt joint and interior of the simple transition.

3. Finite Element Analysis

Finite element models of the three joint configurations, depicted in Fig. 1, were created to study the development of the stress state at the composite/monolith interface. In all cases, the fibers are aligned along the length of the specimen and coincide with the tensile axis for all configurations. Initial work on the butt joint geometry included a full three-dimensional analysis intended to more carefully probe edge effects. The mesh consisted of 2816, 20-noded quadratic brick elements (C3D20) arranged in an 8 by 8 grid within the composite ends and refined to an 8 by 32 grid in the metal interlayer. Uniform displacements were applied in the *y* direction along the top plane of nodes, while the node set which defined the specimen bottom was constrained against both transverse and axial motion. As the full three-dimensional model gave similar results to a less computationally intensive plane strain analysis, the work on the simple and taper transitions was restricted to the

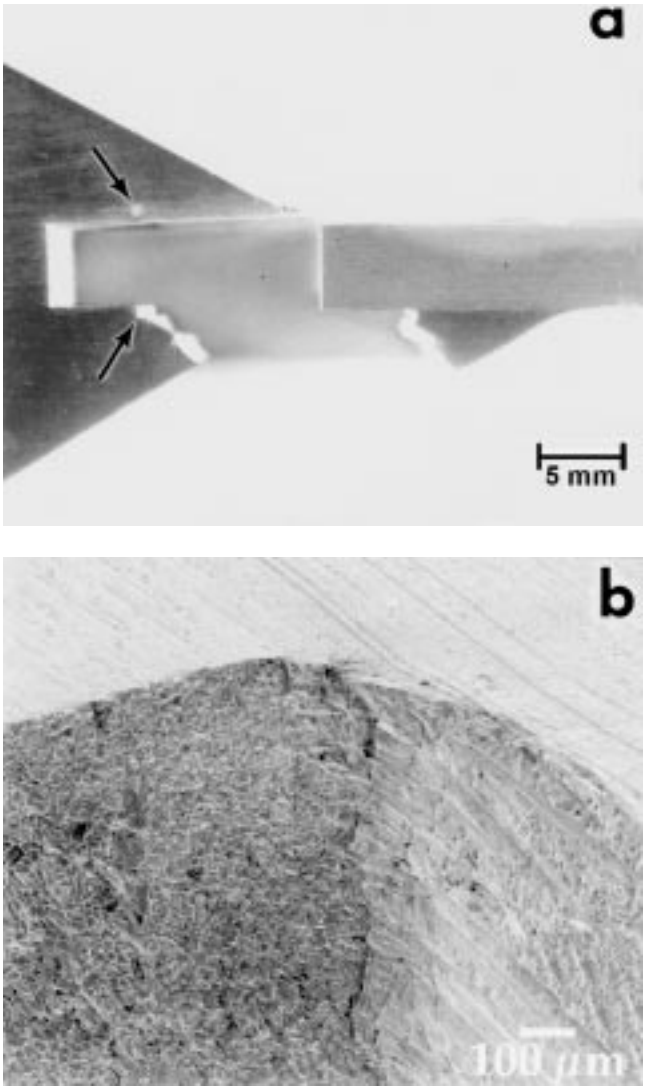

Fig. 7 (**a**) An overview of the fractured transition sample and (**b**) a close-up of the upper corner of the interface region. The arrows in (a) reveal the positions of ceramic pins used to secure the preform during casting, the lower of which appears to have initiated failure in the metal transition region. Fiber grooves that formed during pullout of the composite can be seen on the right side of (b), while the adjacent side of the fracture surface shows the fiber socket morphology of the butt joint

two-dimensional analysis. The simple transition model is mirror symmetric and consists of 520 plane strain elements (CPE4) arranged in a 20 by 26 array, which is biased toward the interface. The finite element model for the taper transition is also mirror symmetric, containing 3200 plane strain elements (CPE4) with 20 elements at the interface, which are biased toward the composite corner. In all cases, the boundary conditions of the models were set to reflect experimental conditions. In addition, the constitutive behaviors of the composite and metal were incorporated into the calculations as measured independently from experiments,[3] so that the results would facilitate direct comparison with the model joints. The composite is elastic and anisotropic with a longitudinal modulus of 210 GPa

and a transverse modulus of 170 GPa. In contrast, the Al-4.5Mg alloy has a modulus of 70 GPa and shows inelastic deformation at 90 MPa. The UTS of the metal is 190 MPa and is reached at a strain of 9%. The calculations were performed on a Silicon Graphics Origin 200 computer using the ABAQUS™ finite element code.

4. Constraint and the Interfacial Stress State

The interfacial normal stress, largely responsible for debonding phenomena at interfaces,[7] is provided in Fig. 8(a) for the three joint configurations. The interfacial stress distributions are compared at an applied load in the composite of 130 MPa, the approximate failure stress of the simple transition specimens. In all cases, the stresses are calculated along the center ($B = 0$) of the composite/monolith interface normal to the applied load. Note that the average normal stress along the interface for the butt joint and simple transition must satisfy equilibrium and match the applied load. In contrast, the applied load on the taper transition specimen is shared between the normal stresses along the width t and shear stresses along the length l. For this reason, the magnitude of the interfacial normal stresses in the taper transition is approximately 42% of those that develop in the other geometries at the given applied load. This is consistent with the increased load bearing ability of the taper transitions.

Although the simple transition and the butt joint have the same average interface normal stress, the distributions of these stresses are quite different. The stresses in the butt joint are relatively flat at an applied load of 130 MPa and suggest that significant stress concentrations have not yet evolved at the edges of the interface.[2] In contrast, the normal stresses that develop on the interface of the simple transition demonstrate stress concentrations on the order of 100% at the edges. These stress concentrations are likely to initiate debonding in these regions and are in keeping with the reduced load carrying capacity of the simple transition.

The distribution of pressure stress at the composite/monolith interfaces, a critical parameter for void growth,[4,8] is shown in Fig. 8(b) and follows a pattern similar to the normal stress. The interfacial stress in the butt joint is significantly higher than the stresses that develop along most of the interface of the simple transition, although stress concentrations that exist at the edges elevate the stresses in this region to levels near that of the butt joint. The higher "baseline" pressure stress in the butt joint stems from the composite constraint, which fosters the development of large triaxial stresses, as discussed earlier. The pressure stress in the taper transition specimen is lower than that of the other geometries, due largely to contributions to load transfer by the shearing regions.

Plastic flow in metals can also contribute to the growth of voids[9] and is considered in Fig. 8(c) as a function of interface position. The plastic strains at the interface of the butt joint and taper transition were near zero, indicating that voidage driven by plastic flow is unlikely for these configurations at

[2]Interfacial stress concentrations do develop at the interface for higher applied loads, however, as described in Ref 5.

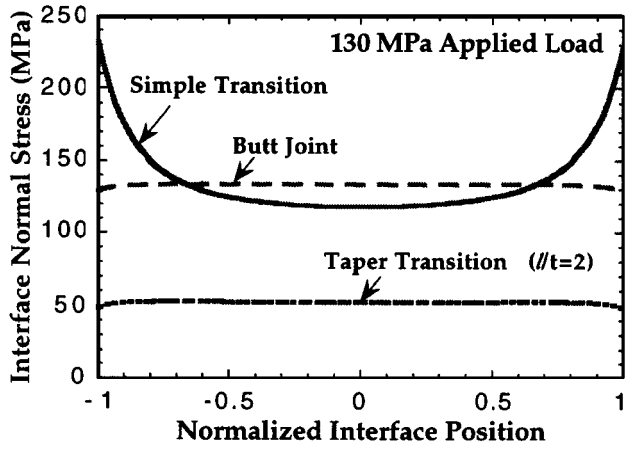

(a)

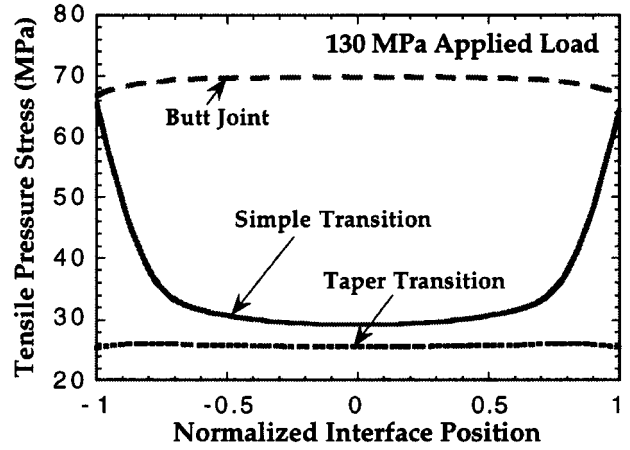

(b)

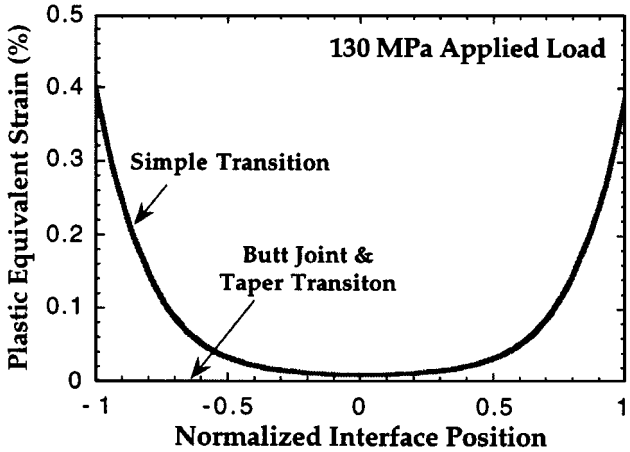

(c)

Fig. 8 Comparisons of the critical components of the stress state, which developed at the composite/monolith interfaces, are given for the various samples at an applied load in the composite of 130 MPa. The (**a**) interface normal stress effects debonding, while the (**b**) pressure stress and (**c**) plastic strain control void growth. The magnitudes of these stresses are consistent with failure in the experimental samples

an applied load of 130 MPa. (Higher applied loads do cause plastic strains to develop for both geometries.) Plastic strains at the interface of the simple transition are significant, however, reaching values of 0.4% at the specimen edges. These large plastic strains agree well with the fracture surface morphology shown in Fig. 5 and are consistent with the reduced failure stresses of these samples.

5. Concluding Remarks

The manufacture and testing of various joint configurations have shown that mechanical performance is limited by the behavior of composite/monolith interfaces normal to the applied load. In addition, the results indicate that geometry has a significant impact on the load bearing ability of these interfaces. This effect stems largely from the degree to which plastic flow is constrained at the composite/monolithic interface, which, in turn, influences void growth and debonding—the observed interfacial failure mechanisms. It is important to note, however, that geometric changes can enable load transfer through shear and contribute to the increase in mechanical performance in this way. Using finite element analysis of the various geometries, the stress state which developed at the composite/monolith interfaces was determined and the extent of plastic flow at the interfaces was quantified. The interfacial normal and pressure stress were also probed, demonstrating that the evolution of these stresses is consistent with the failure mechanisms operating in the experimental specimens.

Acknowledgments

This investigation was sponsored by the National Science Foundation, Mechanics and Materials Program, under Grant No. CMS-9634927. The assistance of Dr. James Yang with melt infiltration, Dr. Ming He in executing the ABAQUS™ finite element code, and Dr. Claus Jeppesen for his computer expertise is gratefully acknowledged.

References

1. A. Burr, J.Y. Yang, C.G. Levi, and F.A. Leckie: *Acta Metall. Mater.*, 1995, vol. 43(5) pp. 3361-3373.
2. R.W. Messler, Jr.: *Joining of Advanced Material*, Butterworth-Heinemann, Stoneman, MA, 1993, pp. 270-74 and 492-96.
3. D.D. Brink, C.G. Levi, A.C.F. Cocks, and F.A. Leckie: *Acta Mater.*, 1997, vol. 45(7), pp. 2765-75.
4. V. Tvergaard: *Acta Metall. Mater.*, 1991, vol. 39(3), pp. 419-26.
5. D.D. Brink, J.C. Mailand, C.G. Levi, and F.A. Leckie: *Mater. Sci. Eng. A*, 2000, vol. A281, pp. 113-25.
6. S.A. Waltner, D.D. Brink, C.G. Levi, and F.A. Leckie: *Composites Sci. Technol.*, submitted for publication.
7. A.G. Evans and B.J. Dalgleish: *Mater. Sci. Eng.*, 1993, vol. A162, pp. 1-13.
8. J.R. Rice and D.M. Tracey: *J. Mech. Phys. Solids*, 1969, vol. 17(3), pp. 201-17.
9. Frank A. McClintock and Ali S. Argon: *Mechanical Behavior of Materials*, Addison-Wesley, Reading, MA, 1966, pp. 226-330 and 524-27.